

CHAPTER IV I-V CHARACTERISTICS

resistance of the depletion region is higher or lower than the resistance of the amorphous film. On other words, in the bulk-limited case the applied bias drop is mainly across the whole amorphous layer, while in the junction-limited case the applied bias drop is across the depletion regions. Because the resistivity and thickness of the a-Si:H film were about $10^9 \Omega \text{ cm}$ and $1.2 \mu \text{ m}$, respectively, the expected current in the bulk-limited case should be equal to or larger than $3.3 \times 10^{-9} \text{ A}$ at 0.05 V for an electrode area of 0.785 mm^2 . The current at bias voltages lower than 0.05 V seems to be Ohmic in nature, as Smid pointed out,⁴⁾ because the value of I seems to be proportional to V in this voltage region. The observed current, however, is much smaller than $3.3 \times 10^{-9} \text{ A}$. Judging from the magnitude of the current, the current for $V \leq 0.4 \text{ V}$ (close to the built-in potential, V_B) is thought to be limited by the a-Si:H/c-Si heterojunction. The voltage dependence of the junction-limited current can generally be expressed by

$$I = I_0[\exp(AV) - 1] \quad , \quad (4-1)$$

where A is voltage-independent and I_0 is the prefactor independent of the voltage. The forward current seems to be proportional to V in the voltage range lower than 0.05 V because $\exp(AV)$ can be approximately expanded in Taylor's series of $1+AV$. Therefore, the I-V characteristics should be discussed on the basis of the junction-limited current-transport mechanism in the voltage region. There is another evidence that the current flowing through this heterojunction is not an SCLC. According to the SCLC model,⁶⁾ the relationship between I/L and V/L^2 should be independent of the thickness (L) of the a-Si:H film. However, $I/L-V/L^2$ characteristics in this study strongly depended on the thickness, indicating that the SCLC model cannot apply to this heterojunction.

4-3. Forward I-V Characteristics

CHAPTER IV I-V CHARACTERISTICS

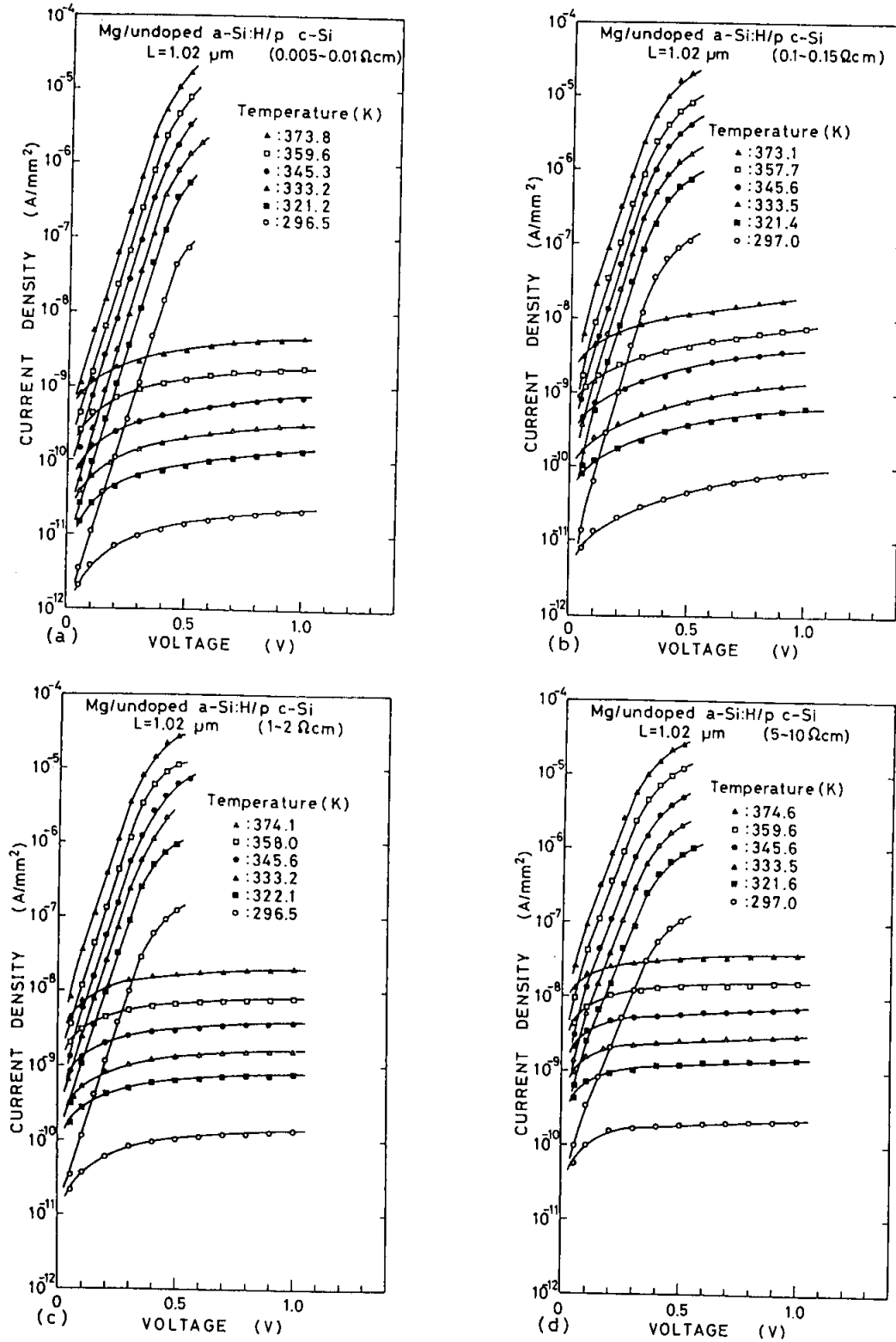


Fig.4.2. I-V characteristics of samples [(a) sample 5, (b) sample 6, (c) sample 7, (d) sample 8] measured at six different temperatures.

CHAPTER IV I-V CHARACTERISTICS

Three kinds of models for explaining the current of heterojunctions, which can be expressed in Eq. (4-1), are discussed:

- (1) A is independent of the measuring temperature (T) for a tunneling model;
- (2) $A=q/kT$ for a diffusion model;
- (3) $A=q/2kT$ for a recombination model.

Samples 5-8 shown in Table 3-1 in Chapter III have been used for studying the I-V characteristics, since the a-Si:H films of 1.02 μm in thickness were deposited simultaneously on p c-Si with four different resistivities; sample 5 (0.005-0.01 Ωcm), sample 6 (0.1-0.15 Ωcm), sample 7 (1-2 Ωcm), and sample 8 (5-10 Ωcm). Their I-V characteristics have been measured as a function of temperature in the range of 297-374 K, but the temperature range scanned in the present work is rather limited. Not only the band-like conduction but also hopping conduction like a variable-range hopping might prevail in the transport of a-Si:H at low temperatures as LeComber et al.⁷⁾ reported that the nearest-neighbor hopping predominated below 240 K. Furthermore, their current below 297 K decreases down to as low as 10^{-12} A, causing another difficulty for measuring accurate currents.

Figure 4.2 shows temperature dependencies of the I-V characteristics of Mg/undoped a-Si:H/p c-Si diodes for samples 5-8, respectively. It is clear from the experimental results that the slope (A) of the forward characteristics is constant for different temperatures; therefore, the current in this voltage region can be described by

$$I = I_0 \exp(AV) \quad (4-2)$$

and

$$I_0 = B_0 \exp(-\Delta E_{af}/kT) \quad , \quad (4-3)$$

where A , ΔE_{af} , and B_0 are temperature- and voltage-independent constants. From Eq. (4-3) the values of ΔE_{af} were estimated to be 0.72, 0.80, 0.65, and 0.63 eV for samples 5-8, respectively.

CHAPTER IV I-V CHARACTERISTICS

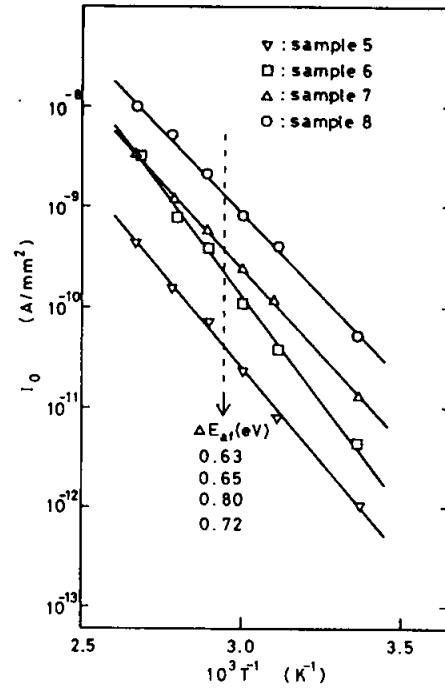


Fig.4.3. Temperature dependence of I_0 of samples 5-8.

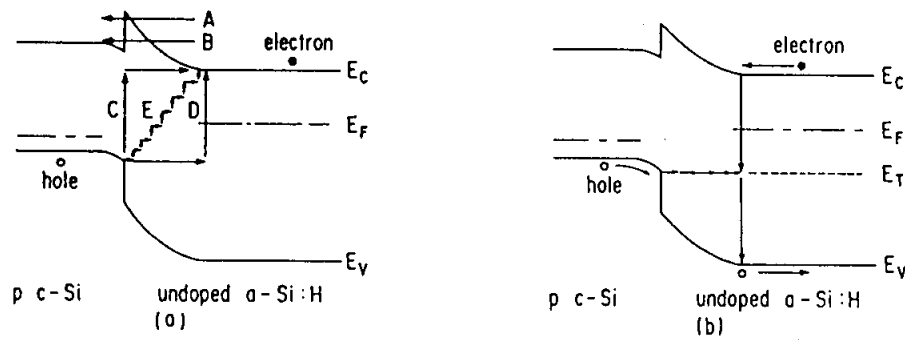


Fig.4.4. Tunneling models for heterojunctions; (a) reported tunneling models and (b) a multistep-tunneling capture-emission (MTCE) model.

CHAPTER IV I-V CHARACTERISTICS

as shown in Fig. 4.3. Since the value of A in Eq. (4-2) is independent of temperature, the forward current must be limited by tunneling.

Models for junction transport based on tunneling processes have been proposed by several groups,^{8,9)} and these are schematically shown in Fig. 4.4(a). To explain the present experimental results, each model is examined separately.

The simplest model consists of the tunneling of carriers through the spike-shaped barrier in the conduction band shown in Fig. 4.4(a). According to Riben,⁹⁾ predominant tunnel flux takes place at an energy close to the peak of the barrier within an energy difference of about 0.1 eV for crystalline heterojunctions, which is indicated by path A in the figure. In the present heterojunction, however, a tunneling process at an energy range far below the barrier peak, indicated by path B in the figure, is quite possible because the gap states are quasi-continuously distributed within the gap of a-Si:H, spatially as well as energetically. The magnitude of ΔE_{af} is expected to be larger than 1.12 eV for sample 5, because at $V=0$ V the difference between the conduction-band edge in p c-Si and the Fermi level in a-Si:H is 1.12 eV, as is clear from Fig. 3.10(a). This requirement contradicts the actual data, i.e., the value of ΔE_{af} for sample 5 was obtained experimentally to be 0.72 eV.

A second model based on the tunneling of carriers was originally presented as the reason for the excess current in tunnel diodes.¹⁰⁾ As was discussed by Riben,^{9,11)} one-step tunneling [C or D in Fig. 4.4(a)] is always smaller than multistep tunneling [E in Fig. 4.4(a)]. The multistep-tunneling process should predominate in the present system because gap states are quasi-continuously distributed in the mobility gap. According to this multistep-tunneling process, I_0 should change exponentially with T due to the temperature dependence of the bandgap.^{9,11)} The value of I_0 obtained in this study, however, varies exponentially with $-1/T$, as shown in Fig. 4.3.

In order to solve this disagreement, a multistep-tunneling capture-emission (MTCE) process has been proposed as the most probable model for the present system, shown in Fig. 4.4(b). A

CHAPTER IV I-V CHARACTERISTICS

hole in the valence band of p c-Si flows from a gap state to another in a-Si:H located in an energy range of kT by a multistep-tunneling process and keeps flowing until the tunneling rate becomes smaller than the rate for hole release from the gap state to the valence band of a-Si:H or the rate for recombination of the hole with an electron in the conduction band of a-Si:H. An ending point of tunneling must be close to the edge of the depletion layer in a-Si:H, since the tunneling rate decreases due to a decrease of the electric field.

Thus, a current flowing from p c-Si to undoped a-Si:H is given by

$$I = B(e_p + \sigma_n v_{th} n) \exp(AV) \quad , \quad (4-4)$$

where B is a constant almost independent of the applied voltage and temperature, σ_n is the capture cross section of electrons, v_{th} is the thermal velocity of electrons, n is the electron density in the conduction band of a-Si:H given by

$$n = N_C \exp[-(E_C - E_F)/kT] \quad , \quad (4-5)$$

e_p is the hole emission rate given as

$$e_p = \sigma_p v_{th} N_V \exp[-(E_T - E_V)/kT] \quad , \quad (4-6)$$

σ_p is the capture cross section of holes, N_V and N_C are the effective densities of states in the valence band and the conduction band of a-Si:H, respectively, and E_F , E_V , E_C , and E_T are the energies of the Fermi level, the top of the valence band, the bottom of the conduction band, and the gap state where the hole combines with an electron or emits into the valence band, respectively. Therefore, the current is described by

$$I = I_0 \exp(AV) \quad (4-2)$$

with

CHAPTER IV I-V CHARACTERISTICS

$$I_0 = B\{\sigma_p v_{th} N_V \exp[-(E_T - E_V)/kT] + \sigma_n v_{th} N_C \exp[-(E_C - E_F)/kT]\} \quad (4-7)$$

By comparing Eqs. (4-3) and (4-7) with the experimental data, several possibilities can be deduced. For the junction property using p c-Si with the lowest resistivity (sample 5), the value of $\Delta E_{af}=0.72$ eV was obtained. This coincides with the activation energy $\delta_2 (=E_C-E_F)$ of the dark conductivity of undoped a-Si:H. Therefore, considering the energy-band diagram shown in Fig. 4.4(b), the electron-capture rate is larger than the hole-emission rate, that is, the second term predominates in the right-hand side of Eq. (4-7). For samples 6-8, on the other hand, the obtained values of ΔE_{af} were 0.80, 0.65, and 0.63 eV, respectively, which correlates with an increase in the substrate resistivity. As is clear from Fig. 3.10(b)-(d), the magnitude of E_T-E_V decreases with an increase in the substrate resistivity. This suggests that the hole emission dominates for these samples, namely, the first term in the right-hand side of Eq. (4-7) determines the magnitude of I_0 . It is in progress that the transition from the electron-capture process to the hole-emission process is discussed in detail.

4-4. Reverse I-V Characteristics

The a-Si:H/c-Si heterojunctions can keep a small dark current even at higher reversed bias range, as shown in Figs. 4.1 and 4.2. From Eq. (4-1), the saturated value of the reverse current is expected to be I_0 . However, the reverse current exceeds the value of I_0 , indicating that the reverse current should be limited by another transport mechanism.

Figure 4.5 shows the reverse current as a function of $(V_B-V)^{1/2}$ for samples 5 and 6 with lower-resistivity p c-Si substrates, which is replotted from the data given in Fig. 4.2(a) and (b), respectively. Figure 4.6 shows the reverse current as a function of $(V_B-V)^{1/2}$ in the larger range of $-5 \text{ V} \leq V \leq -0.5 \text{ V}$,